Original Paper $\sim \sim \sim \sim \sim \sim$

Effects of Forward Cut Length on Tearing Characteristics of Zipper Lines of E-Flute Corrugated Board.

Shigeru NAGASAWA* †, Itaru KOBAYASHI**

To investigate the relationship between the tearing success rate of the E-flute zipper lines and the forward cut length of these zipper lines, the forward cut length was changed in the tearing test while maintaining the connecting portions' length (uncut length) at 3.0 mm, the width of the zipper band at 12.0 mm, and the pulling velocity at 1.0 mm/s. The experimental results show that the tearing success rate of the connecting portions increases with the increase in the forward cut length due to the increasing of the horizontal (in-plane) shear displacement by the vertical (out-of-plane) uplift of the forward cut zone band. The lower and upper complementary-critical lengths of 5.0 and 9.0 mm of the forward cut length, respectively, against the uncut length of 3.0 mm were revealed. Two kinds of bent-dented wrinkles and the corresponding two patterns of the tearing force were observed. These are statistically determined by the crossed (glued) position of the corrugated medium and upper/lower liner against the starting /ending position of the connecting portion.

Keywords: perforation, uplift, machine direction, tearing, upper/lower complementary-critical length, crossed position, starting position

1. Introduction

A zipper band designed for opening a flap of packaging box generally comprises two parallel dashed lines, which are perforations for tearing the zipper band apart¹). The tearing test of the zipper-connecting portions (the uncut zone) of the E-flute corrugated board in the fabrication machine direction was reported by Nagasawa et al. when changing the length of the uncut zone, width of the zipper band, phase shift angle between two dashed lines, and the pulling velocity under conditions of keeping the forward cut length at a=5 mm against the nominal wave length of 3.2 mm of the corrugated layer²). Regarding the failure behavior of tearing of paper, the mode III tear test (out-of-plane shearing), termed as the Elmendorf test³), in which the

tear propagates across the sheet parallel to the direction of the initial slit, is known and standardized (e.g., TAPPI, T414); additionally, the out-of-plane tearing of thin paper using the tensile testing method shows a tearing resistance similar to that in the Elmendorf testing⁴). Such equivalent tearing strength of the E-flute corrugated board was discussed in the previous report²). Although the primary behavior of the tearing test of the E-flute corrugated board was similar to that of the 310 g/m² white-coated paperboard⁵), the upper and lower critical length of the uncut zone a_n =3 mm and 2 mm of the E-flute corrugated board used for determining the success rate of the tearing test²) was affected by the bulging form (uplift) of the forward cut zone, and length of the uncut zone. Herein, the upper and lower critical lengths of the

^{*}Sanjo City University, Faculty of Eng.,

^{**} Nagaoka University of Technology, Dept. of Mechanical Eng.,

[†] Corresponding author, Sanjo City University 5002-5 Kamisugoro, Sanjo, Niigata 955-0091, Japan, TEL:0256-47-5379, FAX:0256-47-5512, Email:nagasawa.shigeru@sanjo-u.ac.jp

uncut zone, at which the tearing success rate of the uncut zone becomes zero and starts to decrease, were defined and used by Nagasawa et al.⁵).

Therefore, in this study, when determining the length of connecting portions (the uncut length) of a_n = 3 mm in the tearing test of the E-flute corrugated board, the length of the forward cut zone (forward cut length) was varied to investigate the deformation behavior of the torn uncut zone and the forward cut zone.

2. Experiment

2.1 Specimens

Fig. 1 shows a schematic of a double-faced corrugated board, that comprises the upper (front side) liner, lower (backside) liner, and the corrugated medium (CM). The general specifications of the prepared E-flute board are as follows: t (board height) =1.5 mm, wave numbers of the CM 93 \pm 5 for 300 mm (wavelength λ = 3.1–3.4 mm); liners' basis weight: 160 g/m²; C5 liners' thickness: 0.220 mm; CM basis weight: 115 g/m²; and, CM thickness: 0.166 mm (JIS P 8118).

Fig. 2 shows the basic layout and size of the specimen for the zipper band tearing test. The parameters of the geometrical pattern of the zipper are as follows: length of dashed- cutting line a (forward cut length) = 2.5, 3.0,

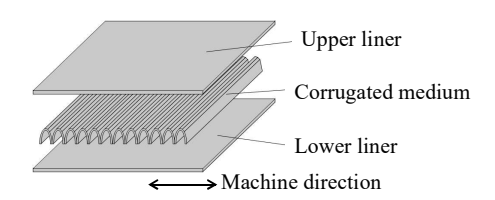


Fig.1 Schematic of the corrugated paperboard

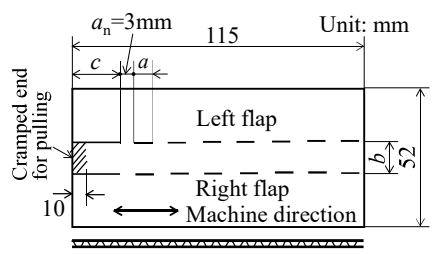


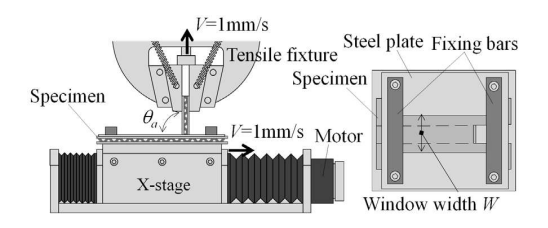
Fig. 2 Specimen layout and size for the tearing test.

3.5, 4.0, 5.0, 6.0, and 9.0 mm; a_n (uncut length) = 3 mm,b (zipper band width) = 12 mm. The band strip comprised two dashed lines of a_n and a. The two-dashed cutting lines were processed using a high-carbon-steel blade (NSK, KG 42417444), that had an angular aperture and crossing angle of 20.5° and 18.4°, respectively. Since the cutting process was two-way, the end profile of the cutting lines was made in the right-angle shape, this processing method was identical to that reported in the previous experiment²). For the clamped end of the band for pulling up, the length of the first cut line c = 30 mm was prepared, and the 10 mm hatched was initially hand-bent at a right angle.

Specimens were prepared in a room at an average temperature of 296 K and relative humidity of 50% for 48 h. The number of specimens was 10 for each zipper pattern (a_n = 3.0 mm, a= 2.5–9.0 mm).

2.2 Experimental method

Fig. 3 shows the experimental apparatus for the tearing test of a corrugated board. The apparatus (**Fig. 3a**) is composed of a uniaxial tensile testing apparatus with pulling velocity V and an X-stage with horizontal moving velocity V. The velocity was set as V=1.0 mm/s. When the specimen was fastened using a window-opened steel plate at b=12.0 mm, the window's width W was set as 20.0 mm (**Fig. 3b**). The angle of the pulling direction θ_a of the zipper band's clamped end was set as 90° against the horizontal X-stage. Due to the restriction of the moving device, the total displacement of the zipper band's clamped end was 35.0 mm. Consequently,



(a) Pulling claw and (b) Fastening X-stage Fig. 3 Schematics of experimental apparatus for the tearing test.

two or three uncut zones (three stages) were torn on the dashed lines of the E-flute specimen when a= 6.0–9.0 mm, and six uncut zones were torn on the specimen at a= 2.5 mm.

In the tearing test, the relationship between the tearing tensile force F and the displacement of the clamped end of the zipper band x was measured for three or more stages of uncut zones. The maximum peak tearing forces F_{pi} (at the stage of i=1,2) were detected from the response. During the process, a digital camera recorded the tearing behavior of the specimen, additionally, the success rate of the separation of the three uncut zones p_S and the failure rate of separation at any stage (i=1-3) p_{Fi} was investigated, except for the case of a=9 mm (due to the restriction of stroke limit). Here, $p_S + \sum_{i=1}^3 p_{Fi} = 1$ for a < 9 mm.

2.3 Fundamental strength of the bending moment

A certain maximum peak-bending moment was experimentally observed when considering a cantilever bending of a band strip in the machine direction. With a 10.0 mm loading position length from the clamped end of a bending strength tester CST-J-1⁶, as shown in **Fig.** 4, the bending moment resistance M (Nmm/mm) of the E-flute corrugated board was measured with respect to the folding angle θ .

Using this bending moment response, the maximum peak-bending moment was investigated, considering the fundamental bending strength at the first stage. For θ > 10°, since the folded-inside liner was buckled at a valley position of the intermediate wave layer, M was lesser than the maximum peak M_{peak} (2.9 Nmm/mm in average) at θ_{peak} (5.2° in an average of five samples)²).

3. Results and discussion

3.1 Fundamental tearing strength

Fig. 5 shows an example of the tearing force F in **Fig. 3** when choosing a long uncut zone ($a_n = 90 \text{ mm}$, a = 0 mm, c = 20 mm).

Half of the maximum peak tearing force $F_{\text{max}}/2 = F_{\text{TS}}$ (the tearing strength of one element) was known as the

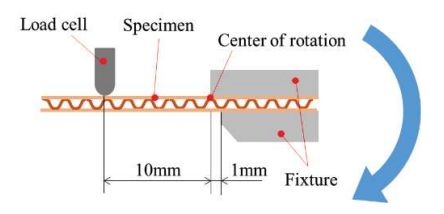


Fig. 4 Schematic of the bending test apparatus.

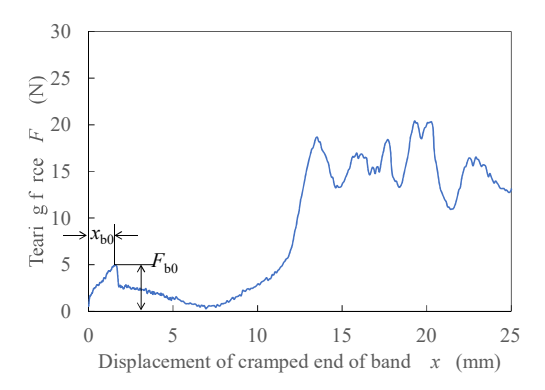


Fig. 5 Representative tearing force response of zipper band when choosing a long uncut zone of 90 mm, with a pulling velocity of 1.67 mm/s, and θ_a = 90°.

average of 10.85 N and with a standard deviation of 0.85 N²⁾. As the early maximum peak, a position of $x_{b0} = 1.5$ mm, $F_{b0} = 4.8$ N was detected (**Fig.5**). Since the arm length of the pulling point was a projection of the bentup band $a_{b0} = \sqrt{((c-10)^2 - x_{b0}^2)} \approx 9.9$ mm, with b=12.0 mm, the bending moment of $F_{b0}a_{b0}$ was determined as $4.8 \times 9.9/12 \approx 4.0$ Nmm/mm, that appears to be equivalent to M_{peak} (= 2.9 Nmm/mm).

3.2 Effect of the forward cut length on the failure state (tearing off)

Fig. 6 shows an example of failure mode after tearing test at a = 3.5 mm. In the tearing test of ten

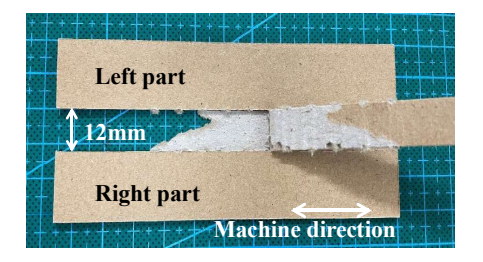


Fig. 6 General view of a failure mode after the tearing test.

samples for each forward cut length, the tearing state was judged as a failure state when any delaminated layer occurred at the lower liner of the band strip in the pull-up process.

Fig. 7 and Fig. 8 show top views of the front side of representative torn uncut zones at the first, second and third stages, and Fig. 9 and Fig. 10 were that at the first and second stages, respectively.



(a) 1st stage (b) 2nd stage (c) 3rd stage

Fig. 7 Top views of the front side, torn uncut zones at = 2.5 mm.

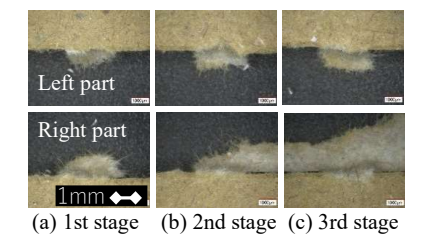


Fig. 8 Top views of the front side, torn uncut zones at = 4.0 mm.

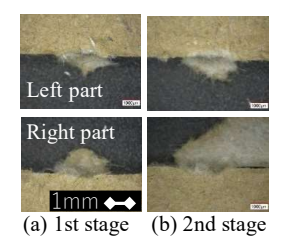


Fig. 9 Top views of the front side, torn uncut zones at = 6.0 mm.

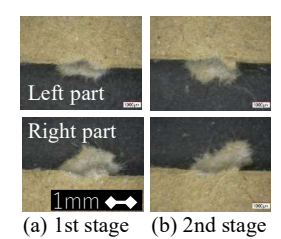


Fig. 10 Top views of the front side, torn uncut zones at = 9.0 mm.

The tearing success rate of uncut zones $p_{\rm S}$ and that of only the first-stage $p_{\rm s1}$ were summarized in **Fig. 11**. The $p_{\rm s1}$ increased with a=3.0-9.0 mm. The success rate $p_{\rm s}$ was judged as zero for a certain short cut length a<5.0 mm, whereas it tended to increase up to 100% for a>5.0 mm. For the case of a=5.0 mm, $a_{\rm n}=3.0$ mm was confirmed to be the same as that in the previous report a=5.0

From the results of a > 5.0 mm (a = 6.0, 9.0 mm), the case of a = 5.0 mm was the starting point of increasing the tearing success rate, whereas the case of a = 9.0 mm (or a slightly lesser length) was detected as the saturated point, with the tearing success rate of 100%. Hence, the success rate of tearing separation was affected by the forward cut length a and the uncut length an when considering the E-flute corrugated board. For convenience, the starting point (the length of a = 5.0 mm against $a_n = 3.0$ mm) for increasing the success rate is termed here as the lower complementary-critical length, while the saturated point (the length of $a \le 9.0$ mm against $a_n = 3.0$ mm) is termed as the upper complementary-critical length.

Fig. 12 shows representative examples of the tearing tensile force F with respect to the displacement x when choosing (a) a=2.5, 3.0 and 3.5 mm and (b) a=4.0, 5.0, 6.0 and 9.0 mm against a_n=3.0 mm.

At the early first stage (x=2-5 mm) in **Fig.12**, the maximum peak force $F_{b0}\approx 4-5$ Nmm/mm was detected. This was explained with **Fig. 4** and **Fig. 5**. This was caused by the out-of-plane bending resistance of the Eflute corrugated board.

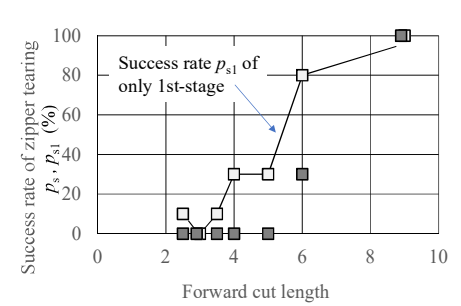
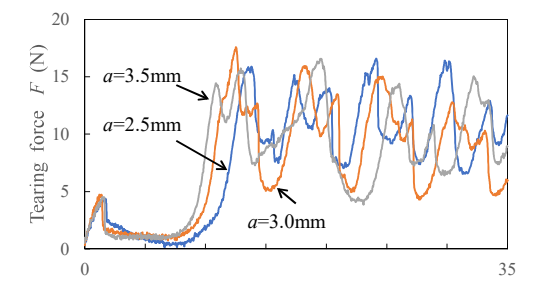
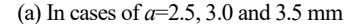
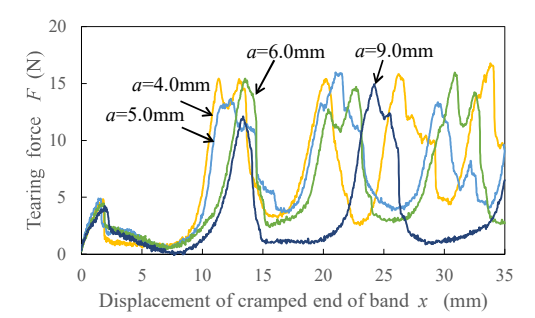


Fig. 11 Success rate of uncut zones' tearing for = 2.5-9.0 mm.







(b) In cases of *a*=4.0, 5.0, 6.0 and 9.0 mm

Fig. 12 Representative relationship between tearing force and displacement of cramped end of the band strip.

After passing the first stage, the first minimum peak force was detected at x=15-18 mm, and similarly the next minimum peak forces were detected in the second, third stages at x>20 mm. Herein, these minimum peak forces tended to decrease with the forward cut length a. Fig. 13 shows the relationship between the first minimum peak force F_{plmin} (at the undershot tearing force after the first stage) and the forward cut length a, derived from Fig.12. Eq.(1) was the linear approximation of these selected figures. Herein, the coefficient of determination R^2 was 0.76.

$$F_{\text{plmin}}(N) = -0.95 \ a \ (mm) + 8.97$$
 (1)

The value of $F_{\rm plmin}$ can be considered to be affected by $F_{\rm b0}$ (the initial bending resistance), the frictional resistance at the zipper lines, and the latecomer bending resistance after bulging (uplift).

Fig. 14 shows the first maximum peak $F_{\rm pl}$ and second maximum peak $F_{\rm p2}$ of tearing force, when selecting a= 2.5, 3.0, 3.5, 4.0, 5.0 6.0 and 9.0 mm against $a_{\rm n}$ =3.0 mm. The average of $F_{\rm pl}$ with a in **Fig. 14** was 15.3 N (69.5%

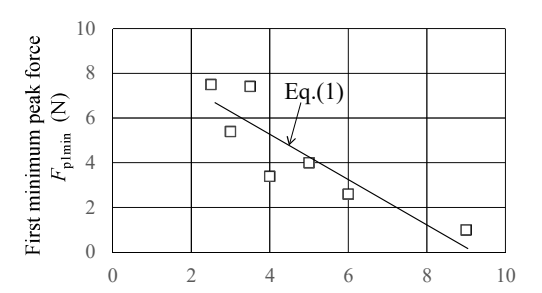


Fig. 13 The first minimum peak force when changing the forward cut length.

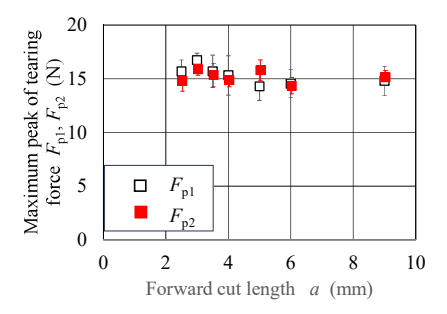


Fig. 14 The first and second maximum peak of tearing force with respect to the forward cut length \approx 2.5, 3.0, 3.5, 4.0, 5.0, 6.0 and 9.0 mm when selecting the uncut length of a_n = 3 mm.

of $2F_{TS}$), and that of F_{p2} with a in **Fig. 14** was 15.2 N (69% of $2F_{TS}$). They are considered to be stable, independent from the variation of a, although increasing a little for a< 5 mm, when fixing a_n = 3.0 mm. According to the previous report²), the tearing peak force was characterized by the use of Eq.(2).

$$F_{\rm p} = 0.50(2F_{\rm TS})(a_{\rm n}/t)^{0.28} \tag{2}$$

In this estimation, when considering t=1.5 mm, F_{TS} =11 N and a_n =3.0 mm, F_p =13.4 N was derived. Although this value was a little lesser than that in **Fig.14**, F_{p1} and F_{p2} appear to be equivalent to this estimation.

Fig.15 shows the failure rate of tearing with respect to the first, second and third stage, except for a=9.0 mm. Here, the definition: $p_S + \sum_{i=1}^3 p_{Fi} = 1$ was explained in Section 2.2. When a < 4.0 mm, the failure of tearing concentrated at the first stage, whereas it distributed in the second and third stages for a=5.0, 6.0 mm. When selecting a=9.0 mm, all cases of tearing succeeded.

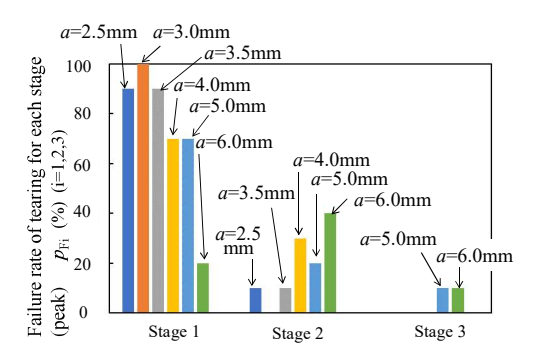


Fig. 15 Failure rate of tearing for each stage.

Considering some force responses in **Fig. 12**, there were mainly two kinds of peak generation: 1) a monotonous maximum peak occurred in a short stroke less than 1.0mm or so, 2) a widely distributed peak that occurred in a stroke of approximately 2.0 or 3.0 mm.

Regarding the third rare case, irregular responses were detected (4 cases, 5.7% of 70 samples). They are recognized as a sort of dispersion of tearing, when the uncut zone matches to or deviates from the crossed (glued) position of the medium and the upper liner of the E-flute corrugated board. Hence, in the following section, the phase effect of the CM against the uncut zone was discussed.

3.3 Phase effect of CM on tearing off

To reveal the difference between the monotonous peak and widely distributed peak, bent and torn zones of dashed lines were observed by a digital microscope at some prominent positions. **Fig. 16** shows representative tearing force responses at the first stage with a=2.5 mm and 9.0 mm. Three positions of the pull-up displacement x at (1), (2), and (3) were noticed near the maximum peak with respect to the monotonous peak and widely distributed peak, respectively. The stroke difference from (1) to (3) was $\Delta x=0.8$ mm at the monotonous peak, while it was $\Delta x=1.8$ mm at the widely distributed peak.

Fig. 17 shows side views of the pull-up band strip at the related positions (1), (2), and (3) to Fig. 16. Herein, (a) shows the monotonous peak, and (b) shows the widely distributed peak, respectively.

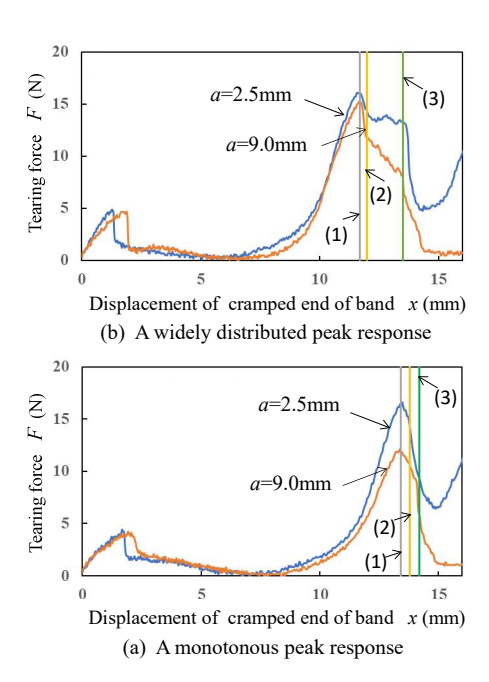
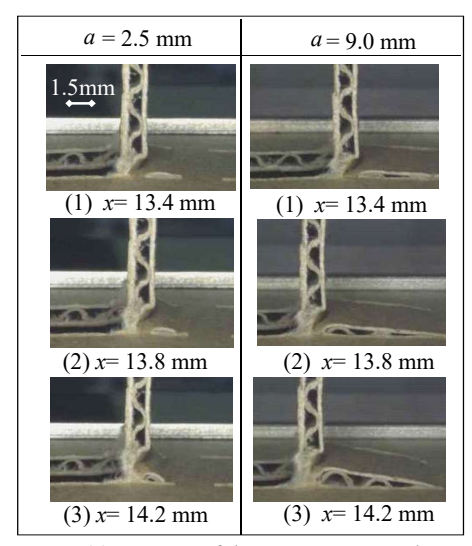


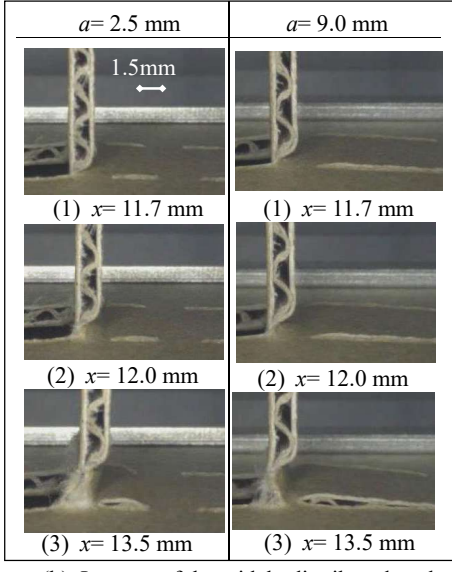
Fig.16 Representative responses of tearing force at the first stage when choosing the forward cut length of \approx 2.5 mm and 9.0mm. (a) A monotonous peak, (b) A widely distributed peak.

Comparing these photographs, the following was observed. (i) At the maximum peak position (1) with the monotonous peak, the torn parts already occurred in both a=2.5 mm and 9.0 mm, whereas there were no torn parts in both a=2.5 mm and 9.0 mm at the maximum peak position (1) with the widely distributed peak. (ii) The peak position (1) of the monotonous peak x=13.4 mm was relatively 13.4-11.7=1.7 mm longer than that of the widely distributed peak x=11.7 mm. Namely, the monotonous peak occurred later than that of the widely distributed peak, because of the constant pulling velocity V=1.0 mm/s. (iii) The uplifted length of a=9.0 mm was larger than that of a=2.5 mm.

After the tearing test, the position of bent-dented wrinkles on the band strip was investigated by observing the surface profile of the wrinkles on the unfolded band strip, except for the third rare case of four samples in 70 samples.



(a) In cases of the monotonous peak



(b) In cases of the widely distributed peak

Fig.17 Side views of the pull-up band strip at the first stage when comparing the forward cut length of a=2.5 mm and 9.0 mm ($a_n=3.0$ mm). See Fig. 16 for referring to the pulling positions (1), (2), and (3).

Fig. 18 shows upper top views of representative unfolded band strips. In Fig. 18, it is observed that the straight(-dented) wrinkle occurred at the left side of the uncut zone (the backward of the torn uncut zone) after the widely distributed peak, while the waved(-dented) wrinkle occurred at the central, right side of the uncut

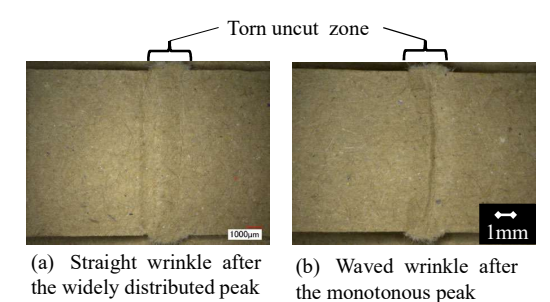


Fig. 18 Upper top views of representative unfolded band strip after the tearing test when *æ* 9.0 mm.

Table 1 Correlation between bent-dented wrinkles and patterns of maximum peak (66 samples for *a*= 2.5-9.0 mm)

	Straight wrinkle %	Waved wrinkle %
Widely distributed peak	51.5	4.6
Monotonous peak	0	43.9

zone (the forward of the torn uncut zone) after the monotonous peak. Herein, the waved wrinkle overlapped the torn uncut zone at the width-end of the band strip.

To confirm the statistical correlation between the wrinkles and patterns of the maximum peak, 66 specimens of the tearing test were inspected. The results of this inspection are summarized in **Table 1**.

Synthetically, it was found that the monotonous peak tended to occur later than the widely distributed peak, due to the difference of the dented wrinkle's position against the torn uncut zone. Namely, the dented wrinkle's position of the monotonous peak existed in the front (forward) of the torn uncut zone, whereas that of the widely distributed peak existed in the rear (backward) of the torn uncut zone.

Since the bent-dented wrinkles were observed to be caused at the weak position against the CM structure, the relation between the starting position of the uncut zone and phase of the medium wave structure was investigated using the four-phase classification shown in Fig. 19. Observing the bent-dented wrinkles after the tearing test, the occurrence rate of the two kinds of wrinkles was listed in Table 2. Herein, 66 samples were

evaluated as the two kinds of wrinkles, while the remaining four samples were excluded as they exhibited irregular patterns (one in the (1) mountain top, three in the (3) first half).

In the case of the mountain top mode, the waved wrinkle frequently occurred, whereas the straight wrinkle was frequently observed in the case of the valley bottom mode. In the case of first half or latter half, the occurrence rate of the two wrinkles was almost even.

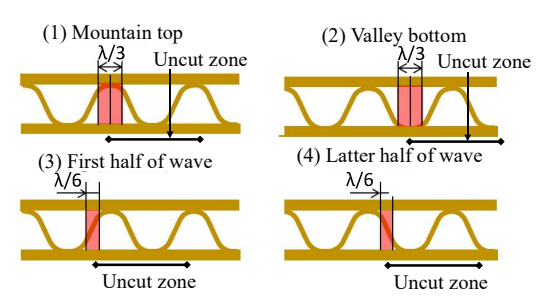
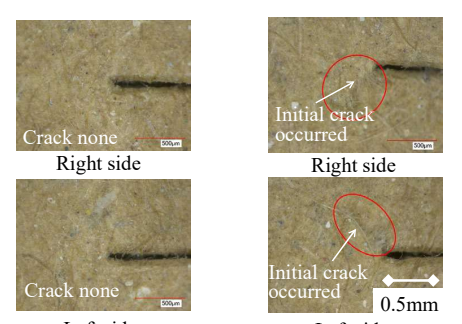


Fig. 19 Four-phase classification of the starting position of the uncut zone in the divided six spans of one medium wave form.

Table 2 Occurrence rate of two wrinkle modes with the classified four-phase conditions (66 samples for *a*= 2.5-9.0 mm). See four phases in Fig. 19.

Phase condition	Subtotal %	Straight wrinkle %	Waved wrinkle %
(1) M.top	30.3	0	30.3
(2) V.bottom	30.3	28.8	1.5
(3) F.half	28.8	18.2	10.6
(4) L.half	10.6	4.5	6.1



Left side Left side
(a) In case of straight wrinkles (b) In case of waved wrinkles

Fig. 20 Back side top views of representative band strips at q_a =80°, a=4.0 mm.

When reaching the maximum peak of the tearing force, the pulling attitude of the band strip is almost θ_a = 90° and the uncut zone starts tearing. Since the event timing when the initial crack generated was not known strictly, the back side of some band strips during the tearing test was observed at $\theta_a = 80^{\circ}$ before reaching the maximum peak. Fig. 20 shows back side top views of representative band strips when a=4.0 mm. The initial cracks were detected on the back side of the lower liner at the attitude of θ_a = 80° in the case of the waved wrinkle, whereas cracks were not detected in the case of the straight wrinkle. From Table 2 and Fig. 19, as the waved wrinkle tends to occur at the phase (1) mountain top mode, the starting point of the uncut zone on the lower liner exists in the weakest supporting condition (without joining any medium wave structure). In contrast, since the straight wrinkle tends to occur at the phase (2) valley bottom mode, the starting point of the uncut zone on the lower liner exists in the strongest supporting condition. Namely, the starting point of the lower liner joins a medium wave structure when considering the straight wrinkle. Thus far, the lower liner of the uncut zone was observed to be easily torn off at the phase (1) mountain top mode, and the monotonous peak was expected in this mode. Here, since the uncut length was fixed as a_n = 3.0 mm ($\approx \lambda$), the end point of the uncut zone was also in the similar supporting condition as shown in **Fig.19.** When considering $a_n \gg \lambda$, the tearing behavior can be considered to be changed.

3.4 Effects of the forward cut length on uplift of the band strip and wrinkle modes

In the previous section, as the occurrence of the waved and straight wrinkle was discussed using **Fig. 19** and **Table 2**, their occurrence was statistically determined by the starting position of the uncut zone.

Fig. 21 shows the relationship between the occurrence rate of the waved wrinkle and forward cut length. As the correlation coefficient of them was -0.22 (the correlation was significantly weak), the occurrence of

the waved wrinkle was almost independent from the forward cut length. From **Fig. 17**, the uplifted deflection of the band strip was remarkable especially for the case of a=9.0 mm. To evaluate the effect of uplift on the tearing deformation, the in-plane shear displacement ΔS , expressed by Eq. (3), was estimated as shown in **Fig. 22**.

$$\Delta S = (S_1 + S_2) - (x + y)$$
 (3)

Measuring the three lengths: h, x and y from the photographs as shown in **Fig. 22b**, the side lengths S_1 and S_2 were calculated by Eq. (4).

$$S_1 = \sqrt{h^2 + x^2}, \ S_2 = \sqrt{h^2 + y^2}$$
 (4)

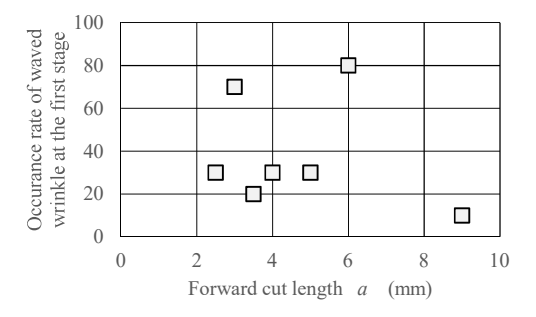
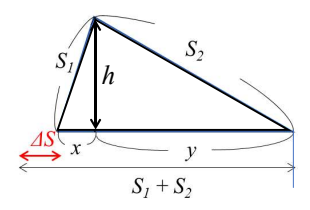
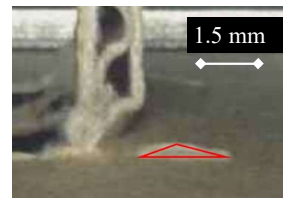


Fig. 21 Occurrence rate of the waved wrinkle at the first stage (10 samples for each cut length).



(b) Geometrical relation between a set of measured data (h, x, y) and the shear displacement ΔS



(a) An example of measuring image (side view of uplift) when a=2.5 mm

Fig. 22 Principle of estimation of uplifted length and the in-plane shear displacement

In a representative case of a=2.5 mm, as h=0.29 mm, x=0.94 mm and y=1.42 mm, then $\Delta S=0.06$ mm was estimated. Similarly, in a representative case of a=9.0 mm, as h=0.41 mm, x=0.98 mm and y=7.50 mm, then $\Delta S=0.09$ mm was estimated. Hence, the inplane shear displacement of a=9.0 mm was 1.5 times larger than that of a=2.5 mm. When the uplift of the band strip is generated, as the in-plane shear deformation contributes to cut off the uncut zone, the forward cut length a=0.0 mm that a=0.0 mm was 1.5 times larger than that of a=0.0

Considering **Fig. 11**, as a > 6.0 mm seems to be stable for tearing off, $a/\lambda > 2$ or a/t > 4 is preferrable.

4. Conclusions

A tearing test of the plain zipper band of an E-flute corrugated board was conducted through two or three stages when changing the forward cut length a=2.5-9.0 mm, while keeping the connecting portions' length (uncut length) at $a_n=3.0$ mm ($a_n/\lambda=0.9-1.0$), the width of the band strip at b=12.0 mm and the pulling velocity at V=1.0 mm/s. The following conclusions were deduced from the experiments.

- (1) For the considered two or three stages, the tearing success rate of the connecting portions (uncut zone) stably increased with *a*> 6.0 mm. Additionally, the tearing success rate at the only first stage remarkably increased with *a*> 3.0 mm.
- (2) The in-plane shear displacement of the uncut zone increases with a due to the out-of-plane uplift of the forward cut zone band. This shear displacement contributes to the tearing off of the uncut zone.
- (3) The lower complementary-critical length (at which the success rate starts to increase from zero) was estimated as a=5.0 mm, and the upper complementary-critical length (at which the success rate reaches or saturates to 100%) was a < 9.0 mm against $a_n = 3.0$ mm.
- (4) When observing the bending deformation of the band strip around the maximum peak tearing force, two kinds of bent-dented wrinkle modes, the

- straight wrinkle and waved wrinkle were detected.
- (5) The maximum peak tearing force was almost classified in two patterns: the widely distributed peak and monotonous peak response.
- (6) Considering the relationship between the wrinkle modes and patterns of the maximum peak force, the waved wrinkle was strongly related to the monotonous peak response, while the straight wrinkle was strongly related to the widely distributed peak response.
- (7) The geometrically crossed position of the CM and the upper/lower liner against the starting/ending position of the uncut zone explains the item (6) adequately.

As a different but similar tearing strip of corrugated carton to the discussed zipper strip, the liner cut structure is well used. To reveal the tearing characteristics of the liner cut structure is furthermore required for some real problems.

9. References

 J.Bota, G.Petković, Evaluation of zipper tear strip design structure for paperboard packaging, Proceedings of International Symposium Graphic Engineering and Design -GRID 2020, At: Novi Sad, Srbija, p.299 (2020).

- S.Nagasawa, K.Ishii & I.Kobayashi, Effects of processing conditions on tearing characteristics of zipper lines of E-flute corrugated paperboard, Journal of Packaging Science & Technology, Japan, 30(6), p.405 (2021).
- M.B.Lyne, M.A.Jackson & A.E.Ranger, The inplane, Elmendorf, and edge tear strength properties of mixed furnish papers, TAPPI, 55(6), p.924 (1972).
- T.Yamauchi, A.Tanaka, Tearing test for paper using a tensile tester, Journal of Wood Science, 48, p.532 (2002).
- 5) S.Nagasawa, M.Uehara & C.Matsumoto, Effects of mechanical conditions on tearing characteristics of zipper band made of white-clay-coated paperboard, Journal of Advanced Mechanical Design, Systems and Manufacturing, 15(1), p. jamdsm0009 (2021).
- 6) Katayama Steel Rule Die Inc., Crease Stress Tester CST J-1 (online), available from http://diemex.com/sale/cst_e.html, (accessed on 23 March, 2024).

(Received: 22 April 2024) (Accepted: 4 July 2024)